Original Article

Use of magnetic resonance imaging in the diagnosis of fetal vertebral abnormalities in utero: a single-center retrospective cohort study

Xianyun Cai[1,2], Xin Chen[2], Xinhong Wei[3], Wen Liu[3], Ximan Hou[1,2], Tao Gong[2], Jinxia Zhu[4], Ewart Mark Haacke[5], Guangbin Wang[1,2]

[1]Cheeloo College of Medicine, Shandong University, Jinan, China; [2]Department of Radiology, Shandong Provincial Hospital Affiliated to Shandong First Medical University, Jinan, China; [3]Department of Ultrasound, Shandong Provincial Hospital Affiliated to Shandong First Medical University, Jinan, China; [4]MR Collaboration, Siemens Healthcare Ltd., Beijing, China; [5]Department of Radiology, Wayne State University, Detroit, Michigan, USA

Contributions: (I) Conception and design: X Cai, X Chen, G Wang; (II) Administrative support: G Wang; (III) Provision of study materials or patients: X Wei, W Liu; (IV) Collection and assembly of data: X Cai, X Chen, X Hou; (V) Data analysis and interpretation: X Cai, X Chen, T Gong, J Zhu; (VI) Manuscript writing: All authors; (VII) Final approval of manuscript: All authors.

Correspondence to: Guangbin Wang. Cheeloo College of Medicine, Shandong University, 44 Wenhuaxi Road, Lixia District, Jinan 250012, China. Department of Radiology, Shandong Provincial Hospital Affiliated to Shandong First Medical University, 324 Jingwuweiqi Road, Huaiyin District, Jinan 250021, China. Email: wgb7932596@hotmail.com.

Background: Magnetic resonance imaging (MRI) has been used increasingly as an adjunct examination to ultrasound (US) for the evaluation of fetal anomalies. The purpose of this study was to determine whether the accuracy and confidence of diagnosing fetal vertebral anomalies are improved with MRI. We also assessed whether fetal MRI provides additional information when diagnosing fetal vertebral anomalies.

Methods: We performed a single-center, retrospective study of 127 pregnant women with fetuses suspected of having vertebral anomalies on US examination; women also underwent fetal MRI scanning. Comparisons of diagnostic accuracy and confidence were made between MRI and US for the identification of fetal vertebral anomalies. We also assessed any additional information provided by MRI. McNemar's paired binomial test, chi-square test, or Fisher's exact test were used to compare the diagnostic ability between MRI and US. In all cases, postnatal or postmortem imaging findings were used as reference standards.

Results: A total of 127 participants were recruited between December 2015 and January 2021. Fetal vertebral anomalies were detected in 63.8% (81/127) cases and found to be negative in 36.2% (46/127) of cases at follow up. The diagnostic accuracy of vertebral anomalies was 46.9% (38/81) for US and 84.0% (68/81) for MRI [difference, 37.1%; 95% confidence interval (CI): 27% to 48%; P<0.001]. Both MRI and US were concordant and correct in 36.2% (46/127) of fetuses; MRI provided additional information for 16.5% (21/127) of fetuses, and corrected US diagnoses of 36.2% (46/127) of fetuses; both MRI and US were not consistent with postnatal findings in 10.2% (13/127) of fetuses, and the remaining fetus (0.8%, 1/127) was diagnosed correctly using US but failed to be diagnosed by MRI. Diagnoses were reported with high confidence using MRI in 95.3% (121/127) of cases and 73.2% (93/127) using US.

Conclusions: Fetal vertebral MRI improves the accuracy and confidence of diagnosing fetal vertebral anomalies. This finding indicates that fetal MRI supplements the information provided by US and that MRI may be a good complement in selected fetuses, when US can either not achieve a definite diagnosis or there is doubt regarding its reliability. Thus, MRI may be used to inform prenatal counseling and management decisions.

Keywords: Fetal imaging; fetal vertebra; ultrasound; fetal vertebral anomalies

Submitted Nov 03, 2021. Accepted for publication Mar 18, 2022.
doi: 10.21037/qims-21-1070
View this article at: https://dx.doi.org/10.21037/qims-21-1070

Introduction

Fetal vertebral anomalies result from abnormal embryonic development during gestational weeks 4–8 (1) and often lead to asymmetric spinal growth, which is classified as congenital scoliosis or kyphosis. The prognosis of fetal vertebral anomalies is related to the type, site, the number of the affected vertebra, and the associated anomalies. Accurate antenatal diagnosis of vertebral anomalies is essential for planning of postnatal follow up to optimize outcomes (2).

Ultrasound (US) is the primary screening method for fetal skeletal evaluation (3). However, certain fetal and maternal factors such as oligohydramnios, advanced gestational age, unfavorable fetal position, maternal abdominal wall scarring, or maternal obesity (4) can undermine the quality of US images. Previous studies have demonstrated a low detection rate in antenatal diagnosis of skeletal anomalies (5-8), especially where there is isolated vertebral involvement without a spinal curvature deformity.

Over the past several years, magnetic resonance imaging (MRI) has been used increasingly as an adjunct examination to US for the evaluation of fetal anomalies (9,10) and has proven useful in imaging fetal spinal canals and cord pathologies (11) with ultrafast spin-echo T2-weighted imaging sequences (12-17). However, literature regarding the use of MRI for the diagnosis of the musculoskeletal system (18-21) and, in particular, bony spinal structures, is scarce and mainly focuses on postmortem imaging examinations without vertebral developmental abnormalities (22-26) or case reports (27,28). Recently, with the improvement and modification of fetal imaging of the susceptibility-weighted imaging (SWI) sequence, the application of fetal MRI for bony spinal structures has attracted mounting attention (29,30). Moreover, at our center (Shandong Provincial Hospital Affiliated to Shandong First Medical University), along with conventional sequences, SWI has been routinely applied to all fetuses suspected of vertebral anomalies on US. In this article, we aimed to compare the accuracy and confidence of diagnosing fetal vertebral anomalies between MRI and US and determine whether MRI can be used successfully as a complementary imaging method in combination with US to optimize prenatal counseling and postnatal management.

We present the following article in accordance with the Standards for Reporting Diagnostic accuracy studies (STARD) reporting checklist (available at https://qims.amegroups.com/article/view/10.21037/qims-21-1070/rc).

Methods

Study population

This retrospective study was conducted in accordance with the Declaration of Helsinki (as revised in 2013) and approved by the Institutional Review Board of Shandong Provincial Hospital Affiliated to Shandong First Medical University. Patients were recruited consecutively, and all participants provided written informed consent. The inclusion criteria was fetuses suspected to have vertebral anomalies on US. The exclusion criteria included women with contraindications to MRI; fetuses without definite follow-up results and incomplete images or poor image quality. A total of 269 second or third trimester pregnant women carrying a fetus with suspected vertebral anomalies (screened by US) were recruited to the study between December 2015 and January 2021. All participants had inconclusive or uncertain findings on US. Of these 269 cases, 128 had no confirmed follow-up results, and 14 cases were excluded, leaving a sample population of 127 fetuses with suspected vertebral anomalies. The participants were then divided into 2 groups: a <28-week gestational age (GA) group (n=68) and a ≥28-week GA group (n=59). The reasons for using a GA of 28 weeks as the dividing point were that problems raised by parents and clinicians at mid-pregnancy needed to be addressed, and image quality improves with GA (30). *Figure 1* shows the selection characteristics of the patients.

Imaging acquisition

The US examinations were performed at the Department of Ultrasound, Shandong Provincial Hospital Affiliated to Shandong First Medical University using a Voluson E10 (GE Healthcare, Waukesha, WI, USA), Philips EPIC 5 or 7 (Philips Healthcare, Best, The Netherlands), or a UGEO WS80A (Samsung, Seoul, Korea) ultrasound unit outfitted with a 3.5–5.0 MHz frequency probe using standard US imaging techniques (31), and static two-dimensional (2D)-US or three-dimensional (3D)-US were used depending on

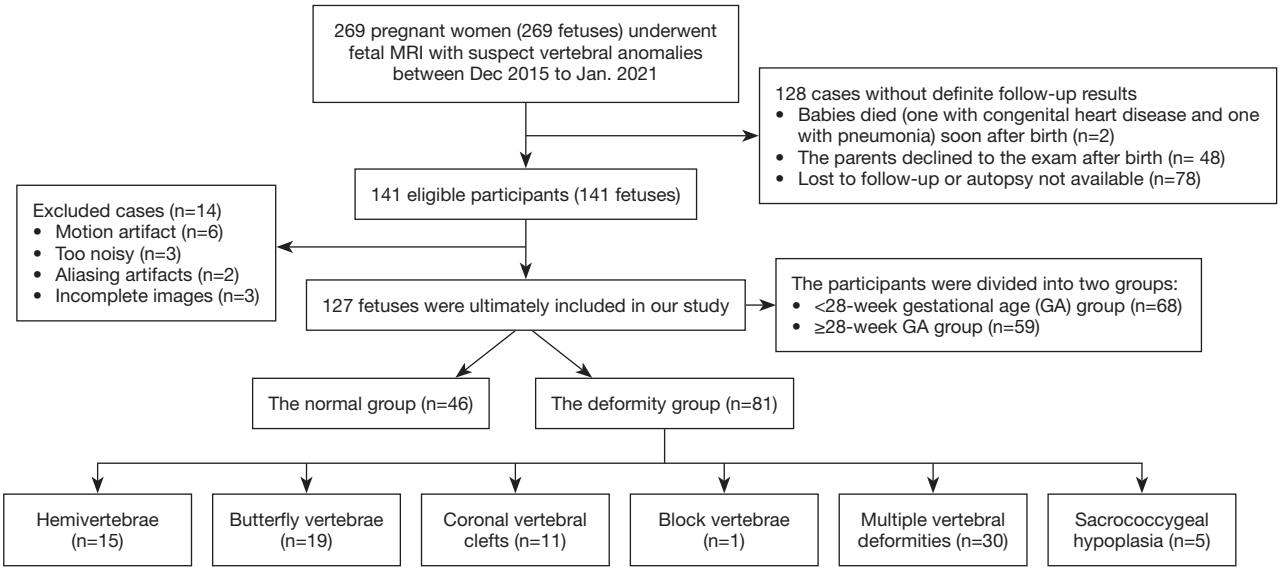

Figure 1 Flowchart of patients with selection data and fetal MRI included in the analysis. MRI, magnetic resonance imaging.

clinical demand. The 3 planes of imaging commonly used to assess the fetal spine from the cervical region through the coccyx included the coronal, parasagittal, and transverse planes. In the transverse plane, it was stipulated that all 3 ossification centers should be visualized, and the centers of the neural arches should be parallel or converging (31). The parallel configuration is particularly noticeable when the fetus is in a decubitus position with respect to the transducer (32). In the longitudinal plane, the spine has a 'railroad track' appearance, with gradual widening towards the fetal head and gradual tapering in the sacrum (33). Fetal MRI examinations were performed within 3 days of the anomalous US findings. All MRI examinations were performed on a 1.5-T MAGNETOM Amira (Siemens, Shenzhen Magnetic Resonance, Ltd., Shenzhen, China) with an 18-channel spine coil and a 13-channel body coil positioned over the lower pelvic area. All cases were imaged in the supine or left-lateral position. The MRI protocol for fetal spine imaging consisted of 2D half-fourier acquisition single-shot turbo spin echo (HASTE), true fast imaging with steady-state (TrueFISP), SWI in 3 orthogonal planes, and a T1-weighted ultrafast sequence in at least one plane (usually sagittal). The SWI was performed immediately after the HASTE or TrueFISP sequences by simply copying the slice position to reduce the chance of fetal motion.

The imaging parameters for the HASTE, TrueFISP, and SWI sequences were as follows: (I) HASTE: repetition time/echo time (TR/TE) =1,300/93 ms; flip angle =180º; field of view (FOV) =308.8 mm × 380 mm; matrix =198×256; bandwidth =698 Hz/pixel; slice thickness =4.0 mm; gap =0; number of slices =15; spatial resolution =1.5 mm × 1.5 mm × 4.0 mm; acquisition time =21 s; and free breathing. (II) TrueFISP: TR/TE=4.06/1.76 ms; flip angle =79°; FOV =310 mm × 380 mm; matrix =198×304; bandwidth =685 Hz/pixel; slice thickness =4.0 mm; gap =0; number of slices =20; spatial resolution =1.3 mm × 1.3 mm × 4.0 mm; acquisition time =12 s; and free breathing. (III) SWI: TR/TE =85/12.40 ms; flip angle =15°; FOV =244.8 mm × 300 mm; matrix =166×256; bandwidth =80 Hz/pixel; slice thickness =3.0 mm; gap =0; number of slices =8; reconstructed spatial resolution =0.6 mm × 0.6 mm × 3.0 mm; acquisition time =26 s; and two breath-holds, each over a period time of 13 s. The entire MRI examination, including setup, was completed within 30 min. No fetal or maternal sedation was used for any of the examinations, and specific absorption rate limits were at or below the recommended levels.

Outcome reference diagnoses

The results of postnatal or postmortem imaging [including X-ray, computerized tomography (CT), and MRI] were considered the diagnostic gold standard for US and MRI detection of vertebral anomalies. Whenever possible, MRI scans or X-rays were performed during follow up to avoid further radiation exposure, except when multiple vertebral malformations required 3D CT reconstruction for a

definitive diagnosis. The MRI examinations of the spine were performed on a 3.0-T system (MAGNETOM Skyra, Siemens Healthcare, Erlangen Germany) or 1.5-T system (MAGNETOM Amira, Siemens Healthcare, Germany). The imaging protocols included T2-weighted imaging (T2WI) in the axial, coronal, and sagittal planes and T1-weighted imaging (T1WI) in the sagittal plane. Spinal CT examinations in cases (supine position) suspected of spinal deformities were performed on a 128-channel, dual source, multidetector-row CT scanner (Siemens Definition Flash, Siemens Healthcare, Germany) as per standard of care. Normalized effective doses for all cases were determined from dose length product (DLP) using conversion factors for CT imaging of the trunk (children >1 to <3 years, 0.028; ≤1 year, 0.044) (34).

Image interpretation and diagnostic accuracy

For fetal vertebral anatomical orientation, the most caudal fetal rib corresponded to the T12 level (35), and the superior aspect of the iliac crest corresponded to the L5 level (35).

All fetal MRI images were assessed by 2 radiologists (** and **, with 5 and 10 years' experience in prenatal and pediatric radiology, respectively), who were blinded to the postnatal results. The US studies were interpreted by 2 sonographers (** and **, with more than 15 years' experience in the prenatal diagnosis of congenital anomalies, respectively). Postnatal or postmortem images were assessed by ** and ** (both with 5 years' experience in prenatal and pediatric radiology). Discrepancies were resolved through consensus. The radiologists were made aware of the diagnoses from US results before the fetal MRI study was completed. In cases with multiple anatomical diagnoses, all diagnoses had to be reported accurately in imaging interpretation to be classified as correct. The diagnostic accuracies for US and MRI studies were determined using the following equation:

$$Accuracy = \frac{(true\ positives + true\ negatives)}{Total\ number\ of\ cases} \quad [1]$$

where true positives and negatives were established at follow-up assessments.

Diagnostic confidence

Assessment of diagnostic confidence in this study was purely descriptive. The level of confidence for each diagnosis of a vertebral anomaly was determined using a 5-point Likert scale (36): "very unsure" (10% certain), "unsure" (30% certain), "equivocal" (50% certain), "confident" (70% certain), and "highly confident" (90% certain). Assessments of the diagnostic confidence were performed by comparing the level of confidence of an US diagnosis and a fetal MRI diagnosis with the accuracy of diagnosis obtained from follow-up examination. Diagnostic confidence of the dominant diagnosis from the MRI and US images (that most likely to influence prognoses) derived from the Likert scales were converted to high confidence (70% and 90%) or low confidence (10%, 30%, and 50%) (37).

Statistical analysis

Statistics analyses were conducted using the software package SPSS 22.0 (IBM Corp., Armonk, NY, USA). Diagnostic accuracy was calculated for both GA groups (<28 and ≥28 weeks) and for the sample as a whole with a McNemar's paired binomial test. Diagnostic accuracies were compared between MRI and US for the subgroups using a chi-square test or Fisher's exact test. A P value (2-tailed) of less than 0.05 was considered to indicate a significant difference.

Results

Participant characteristics

Paired MRI and US data were available with follow-up results for 127 of the pregnant women in this study. The possible non-random sample of cases without follow-up results (n=128) favored either modality (MRI or US), and 14 cases were excluded because of incomplete MRI images or poor image quality, which contributes to bias in the case of US. Of the 127 pregnant women, 116 cases carried pregnancies to term (mean GA, 28±4 weeks), and 11 cases resulted in a termination of pregnancy (mean GA, 27±3 weeks). Characteristics of the study population are shown in *Table 1*.

Follow-up results and diagnostic performance

Postnatal and postmortem imaging results confirmed that 36.2% (46/127) of the fetuses had normal vertebra (*Figure 2A-2F*), and 63.8% (81/127) had vertebral anomalies at follow up. The 81 specific vertebral anomalies included

Table 1 Characteristics of the study population

Characteristics	Follow-up results available (n=127)	Follow-up results unavailable (n=128)	Excluded cases (n=14)
Maternal age at diagnosis (years)	29.8 (4.3)	27.6 (4.5)	25.8 (3.2)
Gestational age at diagnosis			
Mean age (weeks)	28.2 (3.8)	30.9 (3.2)	24.3 (2.8)
<28 weeks	68 (53.5)	61 (47.7)	10 (71.4)
≥28 weeks	59 (46.5)	67 (52.3)	4 (28.6)
Fetal presentation			
Head	101 (79.5)	100 (78.1)	13 (92.9)
Breech	25 (19.7)	28 (21.9)	1 (7.1)
Transverse	1 (0.8)	0	0
Pregnancy options			
Continued pregnancy	116 (91.3)	50 (39.1)	9 (64.3)
Termination of pregnancy/lost to follow up	11 (8.7)	78 (60.9)	5 (35.7)
Age at follow up			
Postnatal age at imaging (years)	2.3 (1.4)	–	–
Postmortem age at imaging (weeks)	26.5 (3.8)	–	–
US site			
Our center	84 (66.1)	90 (70.3)	10 (71.4)
Other centers	43 (33.9)	38 (29.7)	4 (28.6)

Data are mean (SD) or n (%). US, ultrasound; our center refers to Shandong Provincial Hospital Affiliated to Shandong First Medical University.

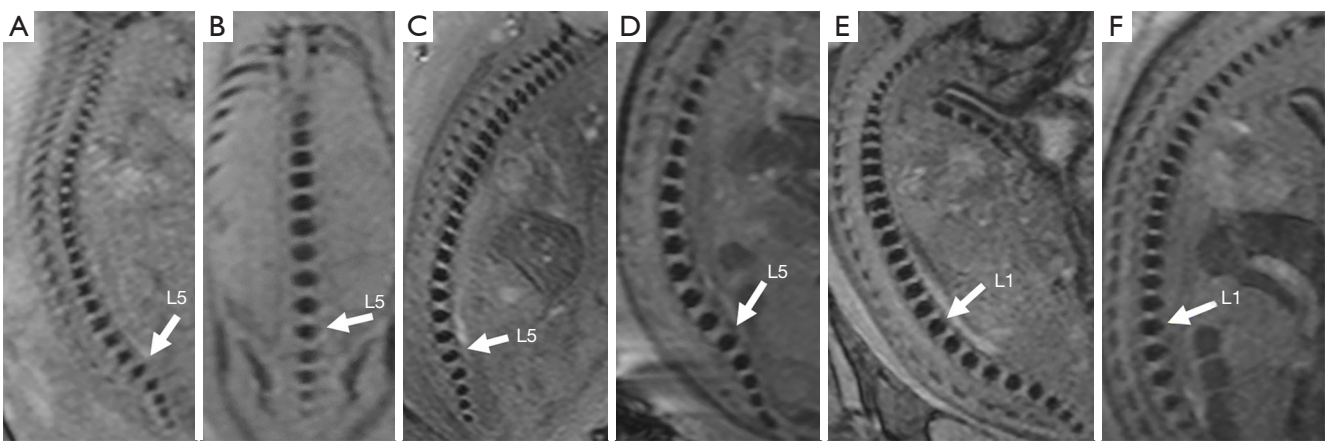

Figure 2 Fetuses with normal vertebral structures. (A) Case 36, 24 weeks; (B) Case 32, 26 weeks; (C) Case 26, 29 weeks +5 d; (D) Case 97, 31 weeks +1 d; (E) Case 43, 34 weeks +6 d; (F) Case 27, 36 weeks. SWI images showed excellent depiction (anatomical location indicated by the arrows) between the bone and surrounding soft tissues, and image quality appears to be improved with increasing gestational ages. SWI, susceptibility-weighted imaging.

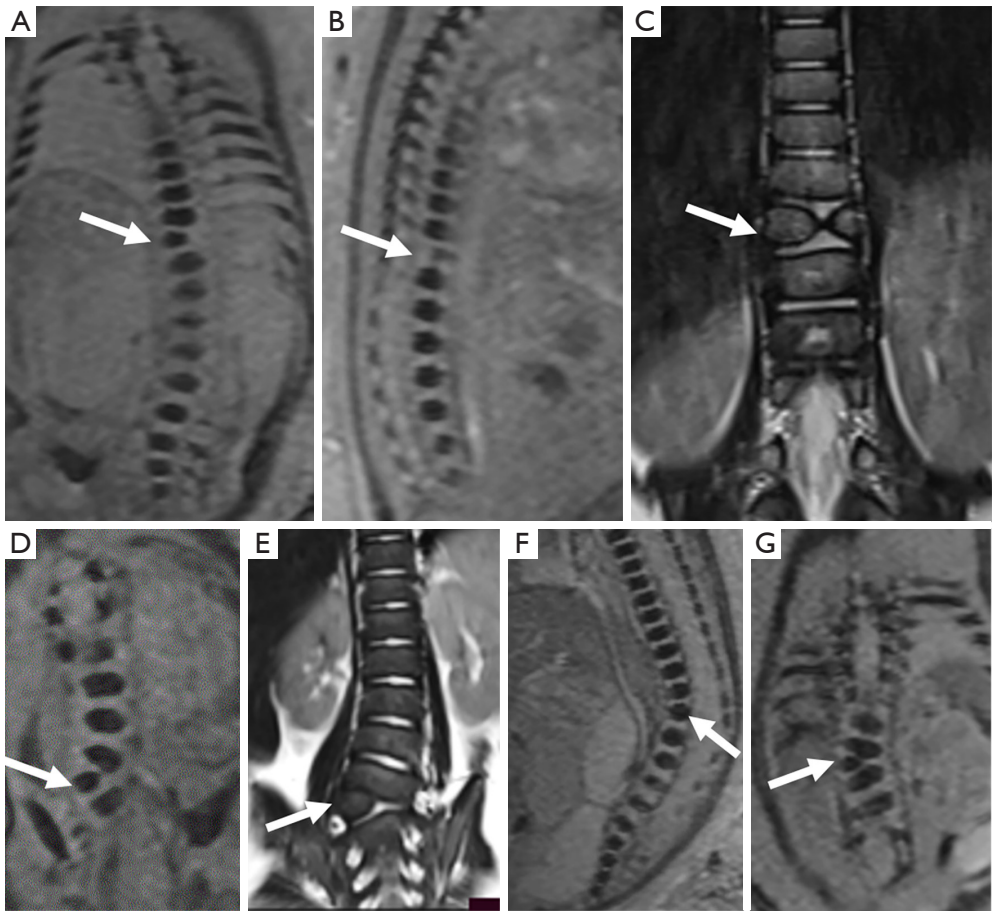

Figure 3 Fetuses with vertebral anomalies. (A-C) Case 56, 31 weeks, T11 was wedge-shaped in coronal and sagittal SWI images (A, B, arrows), diagnosed hemivertebra on prenatal MRI and proved to be butterfly vertebra (C, arrow) at 3 years on postnatal coronal T2WI; (D-E) Case 101, 33 weeks, L5 hemivertebra on prenatal MRI (D, arrow), consistent with postnatal coronal T2WI (E, arrow) at 7 months; (F-G) Case 96, 39 weeks, fetus suspected sacrococcygeal vertebra irregularity in morphology by US showed L2 hemivertebra (G, arrow) with kyphosis (F, arrow) in SWI images. SWI, susceptibility-weighted imaging; MRI, magnetic resonance imaging; T2WI, T2-weighted imaging.

46 isolated vertebral anomalies: butterfly vertebra (n=19) (*Figure 3A-3C*), hemivertebra (n=15) (*Figure 3D-3G*), coronal clefts vertebra (n=11) (*Figure 4A-4C*), block vertebra (n=1) (*Figure 4D-4F*); 30 multiple vertebral anomalies (*Figure 5A-5E*); and 5 sacrococcygeal hypoplasias (*Figure 6A-6E*). Among these, 13 cases had coexisting anomalies: filum terminale (n=1), syringomyelia (n=1), imperforate anus (n=2), meningocele (n=1), congenital undescended scapula syndrome (n=1), caudal degeneration syndrome (n=5), segmental spinal dysgenesis (n=1), and scoliosis (n=1).

The diagnostic accuracy of US and MRI was 46.9% (38/81) and 84.0% (68/81), respectively, in the deformity group, 19.6% (9/46) and 97.8% (45/46), respectively, in the negative group, and 37.0% (47/127) and 89.0% (113/127), respectively, in the overall population. Using MRI, diagnostic accuracy was significantly improved by 33.3% in the <28-week group and by 41.6% in the ≥28-week group (P<0.001) in the deformity group. The same was true for the negative group and the overall sample (both P<0.001). Moreover, the diagnostic accuracy of US in the <28-week GA group was higher than in the ≥28-week GA group in all groups, but the difference was not statistically significant (P=0.397, 0.892, 0.710, 0.312, 0.296, and 0.775, respectively) (*Table 2*). In the subgroup-specific analysis of the anomalies detected using US compared with MRI, the accuracy of the MRI diagnoses was significantly higher than those of the US diagnoses in isolated vertebral anomalies (P<0.001), hemivertebra

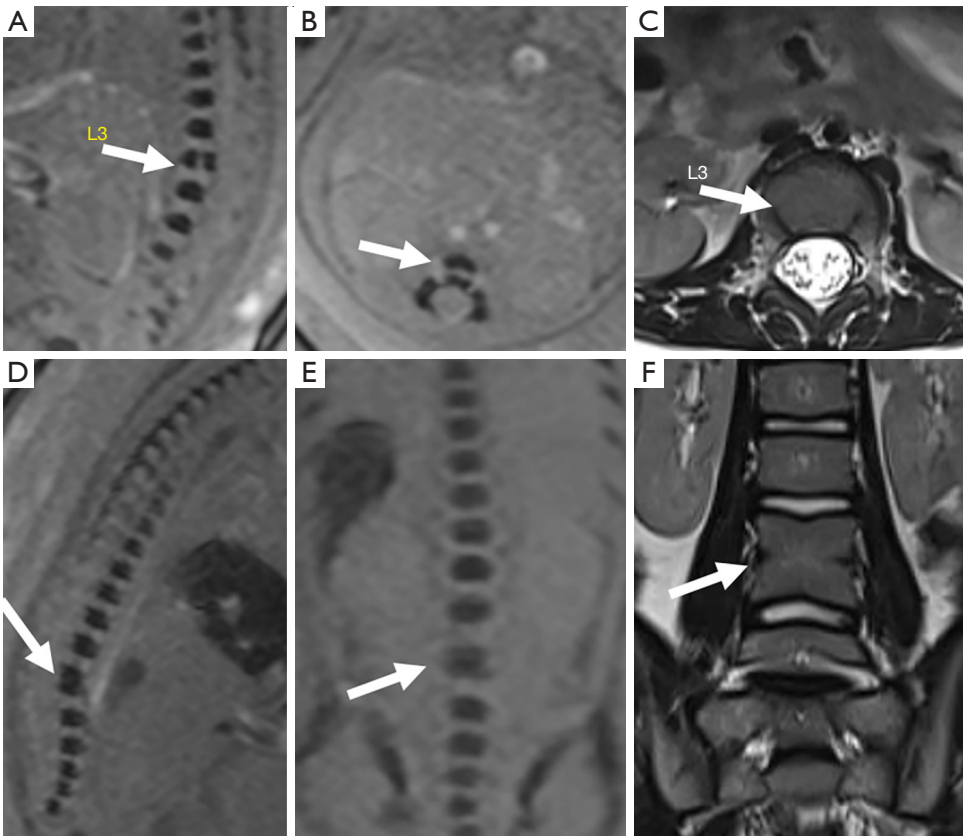

Figure 4 Fetuses with vertebral anomalies. (A-C) Case 72, L3 coronal vertebral cleft at 25 weeks +6 d, demonstrated as a hyperintensity cleft band in sagittal (A, arrow) and axial (B, arrow) SWI images. Postnatal axial T2WI (C, arrow) showed cleft disappear at 7 months; (D-E) Case 90, L3-4 block vertebra at 25 weeks +3 d in sagittal (D, arrow) and coronal (E, arrow) SWI images, corresponding to postnatal coronal T2WI finding (F, arrow) at 10 months. SWI, susceptibility-weighted imaging; T2WI, T2-weighted imaging.

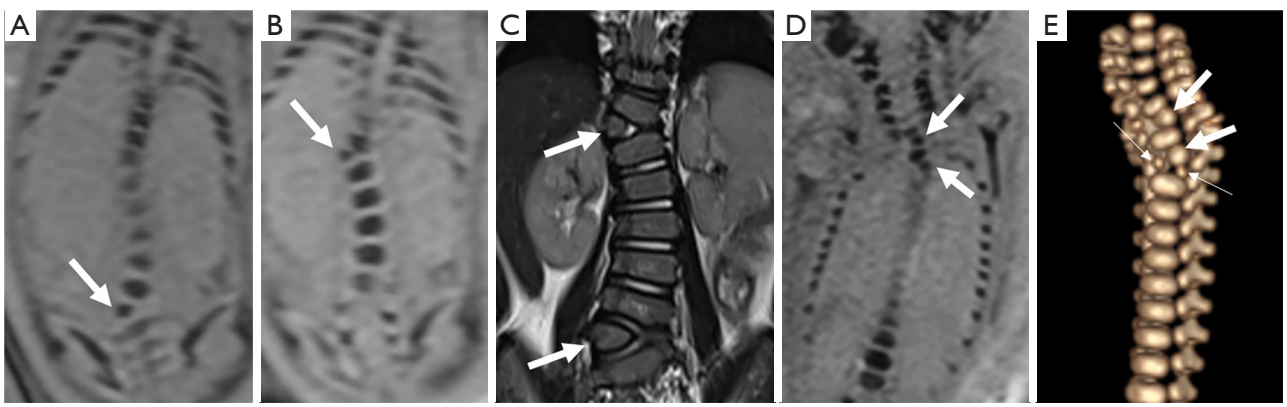

Figure 5 Multiple vertebral anomalies. (A-C) Case 106, L5, T11 hemivertebra at 27 weeks in prenatal coronal SWI images (A, B, arrows), consistent with postnatal coronal T2WI (C, arrows) at 20 months; (D-E) Case 118, C6, T1 hemivertebrae were diagnosed in prenatal coronal SWI at 25 weeks (D, E, thick arrows) and missed diagnosis of T2 butterfly vertebra, which displayed in postmortem CT (E, thin arrows). SWI, susceptibility-weighted imaging; T2WI, T2-weighted imaging; CT, computed tomography.

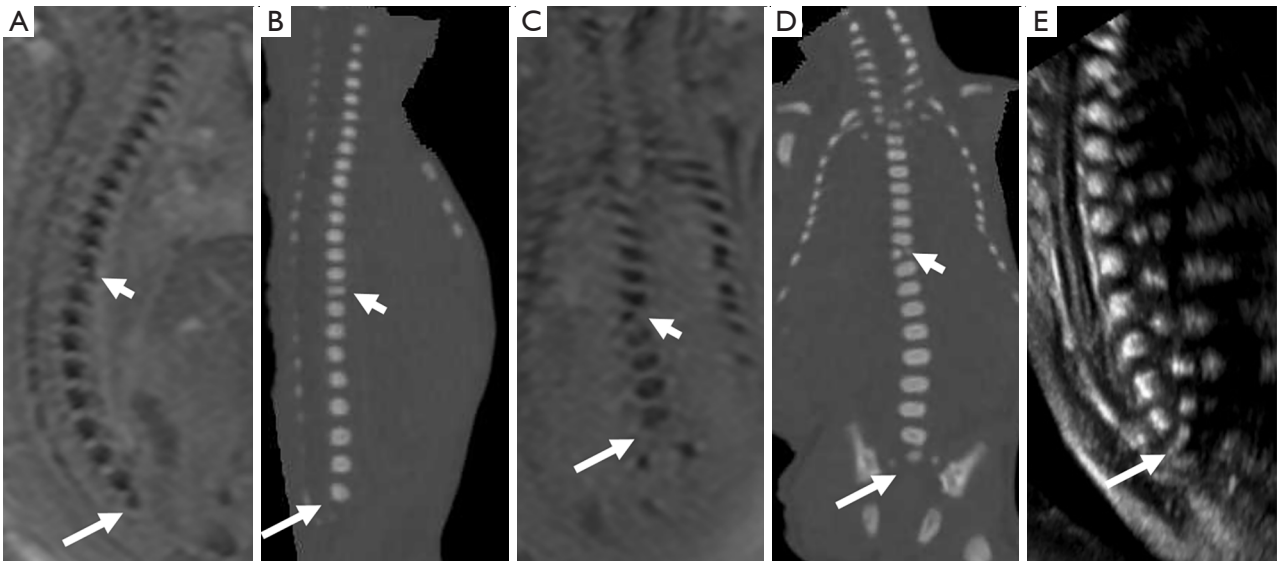

Figure 6 Sacrococcygeal hypoplasia. (A-E) Case 124, (A, C) the spine ends at S1, and the sacrum was not visible below S1 (long arrows) in sagittal and coronal SWI images at 26 w and complicated with T9 hemivertebrae (short arrows). (B, D) These findings were consistent with the postmortem CT (arrows). (E) US shows dysplasia of the sacrococcygeal vertebrae (arrow); however, the T9 hemivertebrae was missed in prenatal diagnosis. SWI, susceptibility-weighted imaging; CT, computed tomography; US, ultrasound.

Table 2 Diagnostic accuracy of ultrasound and fetal magnetic resonance imaging by gestational age in 127 cases

Groups	Gestational age	US correct	MRI correct	Percentage difference (95% CI)	P value* (95% CI)
Deformity group (n=81)	Combined (n=81)	38/81 (46.9%)	68/81 (84.0%)	37.1% (27%, 48%)	<0.001 (0.08, 0.35)
	<28 weeks (n=45)	23/45 (51.1%)	38/45 (84.4%)	33.3% (20%, 47%)	<0.001 (0.07, 0.52)
	≥28 weeks (n=36)	15/36 (41.7%)	30/36 (83.3%)	41.6% (26%, 58%)	<0.001 (0.05, 0.43)
	Percentage difference (95% CI)**	9.4% (–12%, 30%)	1.1% (–15%, 18%)	NA	NA
	P value** (95% CI)	0.397 (0.28, 1.65)	0.892 (0.28, 3.03)	NA	NA
Negative group (n=46)	Combined (n=46)	9/46 (19.6%)	45/46(97.8%)	78.2% (62%, 87%)	<0.001 (0, 0.04)
	<28 weeks (n=23)	5/23 (21.7%)	22/23 (95.7%)	74.0% (48%, 87%)	<0,001 (0, 0.12)
	≥28 weeks (n=23)	4/23 (17.4%)	23/23 (100%)	82.6% (58%, 93%)	<0.001 (NA)
	Percentage difference (95% CI)**	4.3% (–19%, 27%)	4.4% (–10%, 21%)	NA	NA
	P value** (95% CI)	0.710 (0.18, 3.28)	0.312 (NA)	NA	NA
Overall sample (n=127)	Combined (n=127)	47/127 (37.0%)	113 /127 (89.0%)	52.0% (41%, 61%)	<0.001 (0.04, 0.14)
	<28 weeks (n=68)	28/68 (41.2%)	60/68 (88.2%)	47.0% (32%, 59%)	<0.001 (0.04, 0.23)
	≥28 weeks (n=59)	19/59 (32.2%)	53/59 (89.8%)	57.6% (41%, 69%)	<0.001 (0.02, 0.15)
	Percentage difference (95% CI)**	9.0% (–7.8%, 25%)	1.6% (–10%, 13%)	NA	NA
	P value** (95% CI)	0.296 (0.33, 1.41)	0.775 (0.28, 2.61)	NA	NA

*, McNemar's test between US and MRI correct diagnoses. **, Chi-square test or Fisher's exact test between <28 weeks and ≥28 weeks group. US, ultrasound; MRI, magnetic resonance imaging; 95% CI, 95% confidence interval; NA, not applicable.

(P<0.001), coronal clefts vertebra (P=0.011), and multiple vertebral anomalies (P=0.002). The detailed diagnostic accuracy data for the subgroup of fetuses with vertebral anomalies between different modalities within specific GA groups are shown in *Table 3*.

In addition, for the cases with US performed in our center (Shandong Provincial Hospital Affiliated to Shandong First Medical University) (n=84) (*Table 1*), the diagnostic accuracy of MRI was significantly higher than that of US [90.5% (76/84) *vs.* 40.5% (34/84), respectively, P<0.001]; and if the excluded cases (n=14) were included assuming that US could have made the correct diagnosis, the diagnostic accuracy of MRI was significantly higher than that of US [80.1% (113/141) *vs.* 42.6% (60/141), respectively, P<0.001].

In addition, our results showed that MRI and US were concordant and correct in 36.2% (46/127) of cases; MRI yielded findings additional to US in 16.5% (21/127) of cases [butterfly vertebra (n=3), hemivertebra (n=7), and multiple vertebral anomalies (n=11)]; MRI was correct when US failed in 36.2% (46/127) of cases; US was correct and MRI failed in 0.8% (1/127) of cases; both MRI and US were not consistent with postnatal findings in 10.2% (13/127) of cases.

Agreements between US and MRI in the deformity group and the negative group were 45.7% and 19.6%, respectively. A detailed description of agreement and disagreement rates between prenatal US and MRI in different groups is provided in *Table 4*.

After MRI, 116 participants carried pregnancies to term, and 11 participants had a termination of pregnancy. It is worth mentioning that MRI corrected the US diagnosis in 36.2% (46/127) of these cases, including 78.3% (36/46) of the cases where the MRI did not find an abnormality and was justified as correct based on later follow up. In the cases of pregnancy termination, 6 had coexisting anomalies, and 5 had multiple vertebral anomalies.

Of the 10.2% (13/127) cases with incorrect diagnosis using MRI and US, there were 3 cases of butterfly vertebra misdiagnosed as hemivertebra anomalies, 9 cases of multiple vertebral anomalies that were missed or misdiagnosed on MRI, and 1 case (case 46) of a normal vertebra misdiagnosed as a hemivertebra anomaly (*Table 5*). A full summary of all fetal US and MRI imaging findings and follow-up diagnoses is shown in Table S1.

Diagnostic confidence

Figure 7 presents the proportions of correct and incorrect diagnoses made with high and low diagnostic confidence. High-confidence diagnoses were made in 73.2% (93/127) of cases using US compared with 95.3% (121/127) of cases using MRI, an absolute difference of 22%. High-confidence US diagnoses were subsequently found to be incorrect in 44.9% (57/127) of patients compared with 9.4% (12/127) using MRI. The MRI yielded fewer low-confidence diagnoses than US (4.7% *vs.* 26.8%), of which 3.1% (4/127) were found to be correct on MRI, while 8.7% (11/127) were correct on US compared with follow-up results.

Discussion

In this study, we assessed the diagnostic accuracy and confidence of fetal MRI compared to US in 127 fetuses with a range of fetal vertebral anomalies. Several previous studies had used both MRI and US to image the fetal spine (5,38-40), but the sample sizes were small, and the study populations did not focus on fetal spine vertebral malformations. To the best of our knowledge, this is the largest study to date exploring the use of MRI and specifically targeting fetuses with vertebral anomalies. Based on postnatal and postmortem imaging findings, adding fetal MRI to the diagnostic pathway increased diagnostic accuracy to 84.4% for fetuses <28 weeks GA (P<0.001) and to 83.3% for fetuses ≥28 weeks GA (P<0.001). Moreover, MRI provided additional information in 16.5% of the cases. These results indicated that MRI significantly increased the diagnostic accuracy of fetal vertebral pathologies compared to US alone.

Although previous studies assessed fetal skeletal diagnoses and spinal lesions using US or MRI, the diagnostic accuracy ranged from 40.9% to 67.9% (5,6) (7,39,41), and the included populations focused on long bone or spinal canal disease. In our study, we included 127 participants with inconclusive or uncertain fetal vertebral finding on US, where MRI achieved a better diagnostic performance. The higher diagnostic accuracy of MRI (84.0%) compared with US (46.9%) can be explained by the SWI sequence yielding a high contrast between bone and soft tissues but a low contrast between soft tissues (30). Moreover, the higher absolute difference in diagnostic accuracy between MRI and US for the older GA group (41.6%) compared with the younger GA group (33.3%) can be attributed to advancing GA, fetal vertebral body increases in volume, which are increasingly distinguishable from the surrounding soft tissues in SWI images, and amniotic fluid reductions as a result of GA (42) interfering with fetal movement. This increase in vertebral volume and decrease in amniotic fluid

Table 3 Diagnostic accuracy in descriptive categorization of findings between ultrasound and fetal magnetic resonance imaging and different gestational ages

Postnatal/ postmortem final diagnosis	US correct	MRI correct	Percentage difference* (95% CI)	P* (95% CI)	<28 weeks		Percentage difference* (95% CI)	P* (95% CI)	≥28 weeks		Percentage difference* (95% CI)	P* (95% CI)	Percentage difference** (95% CI)	P** (95% CI)	Percentage difference*** (95% CI)	P*** (95% CI)
					US correct	MRI correct			US correct	MRI correct						
Isolated vertebral anomalies (n=46)	25/46 (54.3%)	42/46 (91.3%)	37.0% (19%, 52%)	<0.001 (0.03, 0.37)	17/28 (60.7%)	26/28 (92.9%)	32.1% (10%, 51%)	0.004 (0.02, 0.60)	8/18 (44.4%)	16/18 (88.9%)	44.4% (14%, 66%)	0.005 (0.02, 0.57)	16.3% (–12%, 42%)	0.280 (0.16, 1.72)	4.0% (–13%, 26%)	0.641 (0.08, 4.81)
Butterfly vertebrae (n=19)	12/19 (63.2%)	15/19 (78.9%)	15.8% (–13%, 41%)	0.283 (0.11, 1.94)	10/12 (83.3%)	10/12 (83.3%)	NA	NA	2/7 (28.6%)	5/7 (71.4%)	42.9% (–7%, 72%)	0.109 (0.02, 1.63)	54.8% (9%, 78%)	0.017 (0.01, 0.75)	11.9% (–23%, 49%)	0.539 (0.05, 4.67)
Hemivertebrae (n=15)	7/15 (46.7%)	15/15 (100%)	53.3% (22%, 75%)	<0.001 (NA)	5/9 (55.6%)	9/9 (100%)	44.4% (5%, 73%)	0.023 (NA)	2/6 (33.3%)	6/6 (100%)	66.7% (13%, 90%)	0.014 (NA)	22.2% (–24%, 57%)	0.398 (0.05, 3.42)	NA	NA
Coronal Clefts vertebra (n=11)	6/11 (54.5%)	11/11 (100%)	45.5% (10%, 72%)	0.011 (NA)	2/6 (33.3%)	6/6 (100%)	66.7% (13%, 90%)	0.014 (NA)	4/5 (80.0%)	5/5 (100%)	20.0% (–26%, 62%)	0.292 (NA)	46.7% (–9%, 75%)	0.122 (0.01, 2.0)	NA	NA
Block Vertebral (n=1)	0/1	1/1 (100%)	NA	0.157 (NA)	0/1	1/1 (100%)	NA	0.157 (NA)	0/0	0/0	NA	NA	NA	NA	NA	NA
Multiple vertebral anomalies (n=30)	9/30 (30.0%)	21/30 (70.0%)	40.0% (15%, 59%)	0.002 (0.06, 0.55)	3/14 (21.4%)	9/14 (64.3%)	42.9% (6%, 67%)	0.022 (0.03, 0.81)	6/16 (37.5%)	12/16 (75.0%)	37.5% (3%, 62%)	0.033 (0.04, 0.91)	16.1% (–16%, 44%)	0.338 (0.09, 2.32)	10.7% (–21%, 40%)	0.523 (0.12, 2.89)
Sacrococcygeal hypoplasia (n=5)	4/5 (80.0%)	5/5 (100%)	20.0% (–26%, 62%)	0.292 (NA)	3/3 (100%)	3/3 (100%)	NA	NA	1/2 (50.0%)	2/2 (100%)	50.0% (–27%, 91%)	0.248 (NA)	50.0% (–19%, 91%)	0.171 (NA)	NA	NA

*, comparisons between US and MRI; **, comparisons between <28 and ≥28 weeks in US; ***, comparisons between <28 and ≥28 weeks in MRI. US, ultrasound; MRI, magnetic resonance imaging; 95% CI, 95% confidence interval; NA, not applicable.

Table 4 Rate of agreement and disagreement between prenatal ultrasound and magnetic resonance imaging

MRI *vs.* US	Deformity group (n=81)	Negative group (n=46)	Overall sample (n=127)
MRI and US were concordant and correct	37 (45.7%)	9 (19.6%)	46 (36.2%)
MRI showed additional findings to US	21 (25.9%)	0	21 (16.5%)
MRI correct, US failed	10 (12.3%)	36 (78.3%)	46 (36.2%)
US correct, MRI failed	1 (1.2%)	0	1 (0.8%)
Both MRI and US were not consistent with postnatal findings	12 (14.8%)	1 (2.2%)	13 (10.2%)

Data are n (%). US, ultrasound; MRI, magnetic resonance imaging.

Table 5 Cases misdiagnosed and missed diagnoses using magnetic resonance imaging

Case number	Age (years)	Gestational age (weeks + days)	US findings	MRI findings	Outcomes/follow-up
46	37	25	T11 hemivertebra	T11 hemivertebra	(–)
51	23	27	T10 hemivertebra	T10 hemivertebra	T10 butterfly vertebra
54	38	29	T5 hemivertebra	T5 hemivertebra	T5 butterfly vertebra
56	25	31	T11 hemivertebra	T11 hemivertebra	T11 butterfly vertebra
66	23	32	T1 irregularity in morphology	T1 hemivertebra	T1 hemivertebra; T3 butterfly vertebra
67	31	27	T3, T5, T7, T10 arranged irregularly	T7 butterfly vertebra	T2, T3, T5, T6, T7, T10 butterfly vertebra
				T10 hemivertebra	
110	36	24	T4, T9 hemivertebra	T9 butterfly vertebra	T8, T9 butterfly vertebra
			T8 butterfly vertebra	T4 hemivertebrae	T4, L2 hemivertebrae
			L1-2 block vertebrae	L1-2 block vertebrae	
113	29	21+6	Multiple vertebral deformities; hemivertebra?	T5, T11 hemivertebra	T3, T5, T7, T11 hemivertebra
				T10 butterfly vertebra	T10 butterfly vertebra
				T8-9, L3-4 block vertebra	T8-9, L3-4 block vertebra
114	26	29	T6, T7 hemivertebrae?	T6, T7, T9 hemivertebra and/or butterfly vertebra	T5, T7, T8 butterfly vertebra
					T6 hemivertebra
115	30	24	T11, T12 arranged irregularly	T11-12 block vertebra	T3 hemivertebra
					T4, T8, T9 butterfly vertebra
					T11-12 block vertebra
116	26	31	Cervical vertebral arranged irregularly	Cervical vertebral body and appendix	The congenital undescended scapula syndrome (sprengel deformity)
				Arranged irregularly	Cervical closed spina bifida
118	28	25	Multiple vertebral deformities with scoliosis in upper thoracic	C6, T1 hemivertebra	C6, T1 hemivertebra
					T2 butterfly vertebra
120	23	29	Vertebrae arranged irregularly in lower cervical and upper thoracic	T6-8 block vertebra, and/or hemivertebra	T3 butterfly vertebra
					T5-6, T11-12, L4-5 block vertebra

US, ultrasound; MRI, magnetic resonance imaging.

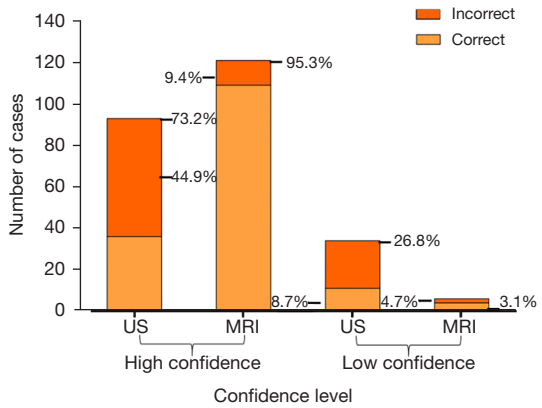

Figure 7 High (rated as 70% or 90%) and low (rated as 10%, 30%, or 50%) confidence diagnoses made using US and MRI in 127 patients in comparison with the follow-up results. US, ultrasound; MRI, magnetic resonance imaging.

contribute to better MRI definitions on image quality but weaken the accuracy of US.

In fetal US examinations, operational bias caused by ongoing ossification of the fetal skull, increasing physical size of the woman, decreasing amniotic fluid, and descent of the fetal head into the maternal pelvis with GA may decrease the diagnostic accuracy of US, especially in the ≥28-week group in certain subgroups. In addition, acoustic shadowing in US from the overlying iliac wing, the scapula, or bones of the fetal arm make it difficult for US views, especially standard coronal views, to demonstrate or there are artifacts, and as such, the fetal sacrum, cervical, and upper thoracic spine may be difficult to view on coronal view (32). However, MRI images can be obtained in any orientation with large FOV and offset the shortcomings of US. The advent of 3D-US has made evaluation of the fetal spine more comprehensive. It allows for evaluation of the complete anatomy of the spine, which is not always possible in 2D imaging due to the curvature of the spine (43). However, given this was a retrospective analysis, 2D-US or 3D-US were alternately used depending on clinical requirements.

Use of MRI provided additional information relative to US in 16.5% of cases, mainly in cases of butterfly vertebra and hemivertebra, which in US are better imaged using coronal views rather than routine sagittal views, as discussed before. Another important finding of our work was that in 36.2% of cases, the US diagnosis was revised by MRI such that management and parental counseling changed completely. Most of these revisions occurred in the negative group (36/46). Moreover, the negative group showed a wide disagreement diagnosis between MRI and US. It is important to understand that this may in part be explained by referral bias, because the participants included in our study were suspected of fetal vertebral anomalies using US instead of negative US.

Of the 81 cases with vertebral anomalies, 16.0% were incorrectly diagnosed by MRI, primarily in cases of butterfly vertebra and multiple vertebral anomalies. Butterfly vertebra results from 2 lateral centers of chondrification failing to fuse at the midline (44). When the bilateral ossification center is asymmetric, the condition can be misdiagnosed (case 56) or result in a missed diagnosis (case 118) by MRI. Moreover, in our study there were 4 cases of partially segmented hemivertebra (cases 91 to 94) diagnosed incorrectly with US but revised with MRI, which was of great importance to prenatal counseling and postnatal management. Hemivertebra could be classified into unsegmented hemivertebra, partially segmented hemivertebra, and fully segmented hemivertebra, on the basis of presence or absence of fusion to the vertebral bodies above and/or below (45). Partially segmented hemivertebra are less likely to cause curvature of the spine with good prognosis during postnatal growth (45) compared with fully segmented hemivertebra (cases 95 to 107). In addition, there were 11 cases of isolated coronal clefts and 11 cases of multiple coronal clefts in our study (cases 68 to 89). The clefts predominantly occurred in the lumbar region (16/22, 73%) and all of these clefts disappeared after birth, consistent with a previous study (46). Hence, coronal clefts in fetuses should not be interpreted as vertebra malformation, but as a physiological variation of vertebral body development. In addition, some diseases with low incidence that involve fetal vertebra, such as osteochondrodysplasias (47) and hypophosphatasia (48), were not encountered in our study.

Several studies have demonstrated the importance of diagnostic confidence in assessing an imaging technology (37,49). Ng and Palmer (50) explained the relevance of diagnostic accuracy and diagnostic confidence. In our study, the proportion of high-confidence diagnoses on MRI increased by 22% compared with US. An incorrect diagnosis made with high confidence can result in an inappropriate change in management, including termination of pregnancy. The MRI resulted in fewer high-confidence, incorrect diagnoses compared with US (9.4% *vs.* 44.9%, respectively) and resulted in fewer low-confidence diagnoses

(4.7% *vs.* 26.8%, respectively).

This study had several limitations. Firstly, the SWI sequence in our study was sensitive to motion artifacts, requiring a breath-hold scan. Often several scans were needed to cover the required volume, particularly for younger GA fetuses; secondly, the retrospective methodology may have led to an underestimation of the diagnostic power of US; thirdly, fetal spinal canal and cord pathologies were not included in our study; and lastly, there was a lack of reported sensitivity or specificity of MRI and US in patients, because cases were derived from abnormal US findings. Future studies should be multicenter, prospective, and randomized controlled design, including spinal canal cases.

Conclusions

Fetal vertebral MRI improves the accuracy and confidence of diagnosing fetal vertebral anomalies. Such improvements are likely to result in changes to counseling and clinical management of spinal anomalies.

Acknowledgments

Funding: This work was supported by the National Natural Science Foundation of China (No. 81671668) and the Natural Science Foundation of Shandong Province (No. ZR2020QH268).

Footnote

Reporting Checklist: The authors have completed the STARD reporting checklist. Available at https://qims.amegroups.com/article/view/10.21037/qims-21-1070/rc

Conflicts of Interest: All authors have completed the ICMJE uniform disclosure form (available at https://qims.amegroups.com/article/view/10.21037/qims-21-1070/coif). EMH serves as an unpaid editorial board member of *Quantitative Imaging in Medicine and Surgery*. JZ is an employee of Siemens Healthcare. The other authors have no conflicts of interest to declare.

Ethical Statement: The authors are accountable for all aspects of the work in ensuring that questions related to the accuracy or integrity of any part of the work are appropriately investigated and resolved. This retrospective study was conducted in accordance with the Declaration of Helsinki (as revised in 2013) and approved by the Institutional Review Board of Shandong Provincial Hospital Affiliated to Shandong First Medical University. All patients gave written informed consent before participating in this study.

References

1. Arlet V, Odent T, Aebi M. Congenital scoliosis. Eur Spine J 2003;12:456-63.
2. Goldstein I, Makhoul IR, Weissman A, Drugan A. Hemivertebra: prenatal diagnosis, incidence and characteristics. Fetal Diagn Ther 2005;20:121-6.
3. Benson CB, Doubilet PM. The history of imaging in obstetrics. Radiology 2014;273:S92-110.
4. Hendler I, Blackwell SC, Bujold E, Treadwell MC, Mittal P, Sokol RJ, Sorokin Y. Suboptimal second-trimester ultrasonographic visualization of the fetal heart in obese women: should we repeat the examination? J Ultrasound Med 2005;24:1205-9; quiz 1210-1.
5. Basude S, McDermott L, Newell S, Wreyford B, Denbow M, Hutchinson J, Abdel-Fattah S. Fetal hemivertebra: associations and perinatal outcome. Ultrasound Obstet Gynecol 2015;45:434-8.
6. Nemec SF, Kasprian G, Brugger PC, Bettelheim D, Amann G, Nemec U, Rotmensch S, Graham JM Jr, Rimoin DL, Lachman RS, Prayer D. Abnormalities of the upper extremities on fetal magnetic resonance imaging. Ultrasound Obstet Gynecol 2011;38:559-67.
7. Schramm T, Gloning KP, Minderer S, Daumer-Haas C, Hörtnagel K, Nerlich A, Tutschek B. Prenatal sonographic diagnosis of skeletal dysplasias. Ultrasound Obstet Gynecol 2009;34:160-70.
8. Abrams SL, Filly RA. Congenital vertebral malformations: prenatal diagnosis using ultrasonography. Radiology 1985;155:762.
9. Frates MC, Kumar AJ, Benson CB, Ward VL, Tempany CM. Fetal anomalies: comparison of MR imaging and US for diagnosis. Radiology 2004;232:398-404.

10. Prayer D, Brugger PC. Investigation of normal organ development with fetal MRI. Eur Radiol 2007;17:2458-71.
11. Simon EM. MRI of the fetal spine. Pediatr Radiol 2004;34:712-9.
12. Glenn OA, Barkovich J. Magnetic resonance imaging of the fetal brain and spine: an increasingly important tool in prenatal diagnosis: part 2. AJNR Am J Neuroradiol 2006;27:1807-14.
13. Nagaraj UD, Bierbrauer KS, Stevenson CB, Peiro JL, Lim FY, Zhang B, Kline-Fath BM. Spinal Imaging Findings of Open Spinal Dysraphisms on Fetal and Postnatal MRI. AJNR Am J Neuroradiol 2018;39:1947-52.
14. Huang YL, Wong AM, Liu HL, Wan YL, Lin YC, Chao AS, Chang YL. Fetal magnetic resonance imaging of normal spinal cord: evaluating cord visualization and conus medullaris position by T2-weighted sequences. Biomed J 2014;37:232-6.
15. Duczkowska A, Bekiesinska-Figatowska M, Herman-Sucharska I, Duczkowski M, Romaniuk-Doroszewska A, Jurkiewicz E, Dubis A, Urbanik A, Furmanek M, Walecki J. Magnetic resonance imaging in the evaluation of the fetal spinal canal contents. Brain Dev 2011;33:10-20.
16. Williams F, Griffiths PD. Spinal neural tube defects on in utero MRI. Clin Radiol 2013;68:e715-22.
17. Egloff A, Bulas D. Magnetic Resonance Imaging Evaluation of Fetal Neural Tube Defects. Semin Ultrasound CT MR 2015;36:487-500.
18. Blaicher W, Mittermayer C, Messerschmidt A, Deutinger J, Bernaschek G, Prayer D. Fetal skeletal deformities - the diagnostic accuracy of prenatal ultrasonography and fetal magnetic resonance imaging. Ultraschall Med 2004;25:195-9.
19. Nemec U, Nemec SF, Weber M, Brugger PC, Kasprian G, Bettelheim D, Rimoin DL, Lachman RS, Malinger G, Prayer D. Human long bone development in vivo: analysis of the distal femoral epimetaphysis on MR images of fetuses. Radiology 2013;267:570-80.
20. Gilligan LA, Calvo-Garcia MA, Weaver KN, Kline-Fath BM. Fetal magnetic resonance imaging of skeletal dysplasias. Pediatr Radiol 2020;50:224-33.
21. Chauvin NA, Victoria T, Khwaja A, Dahmoush H, Jaramillo D. Magnetic resonance imaging of the fetal musculoskeletal system. Pediatr Radiol 2020;50:2009-27.
22. Matsubara Y, Higaki T, Tani C, Kamioka S, Harada K, Aoyama H, Nakamura Y, Akita T, Awai K. Demonstration of Human Fetal Bone Morphology with MR Imaging: A Preliminary Study. Magn Reson Med Sci 2020;19:310-7.
23. Widjaja E, Whitby EH, Paley MN, Griffiths PD. Normal fetal lumbar spine on postmortem MR imaging. AJNR Am J Neuroradiol 2006;27:553-9.
24. Szpinda M, Baumgart M, Szpinda A, Woźniak A, Mila-Kierzenkowska C. Cross-sectional study of the neural ossification centers of vertebrae C1-S5 in the human fetus. Surg Radiol Anat 2013;35:701-11.
25. Jian N, Tian MM, Xiao LX, Zhao H, Shi Y, Li G, Zhang S, Lin XT. Normal development of sacrococcygeal centrum ossification centers in the fetal spine: a postmortem magnetic resonance imaging study. Neuroradiology 2018;60:821-33.
26. Jian N, Lin N, Tian MM, Zhang S, Li G, Zhao H, Xiao LX, Liang WJ, Lin XT. Normal development of costal element ossification centers of sacral vertebrae in the fetal spine: a postmortem magnetic resonance imaging study. Neuroradiology 2019;61:183-93.
27. Westvik J, Lachman RS. Coronal and sagittal clefts in skeletal dysplasias. Pediatr Radiol 1998;28:764-70.
28. Ekim A. Butterfly vertebra anomaly: A case report. J Back Musculoskelet Rehabil 2010;23:161-4.
29. Goodall AF, Barrett A, Whitby E, Fry A. T2*-weighted MRI produces viable fetal "Black-Bone" contrast with significant benefits when compared to current sequences. Br J Radiol 2021;94:20200940.
30. Robinson AJ, Blaser S, Vladimirov A, Drossman D, Chitayat D, Ryan G. Foetal "black bone" MRI: utility in assessment of the foetal spine. Br J Radiol 2015;88:20140496.
31. Budorick NE, Pretorius DH, Nelson TR. Sonography of the fetal spine: technique, imaging findings, and clinical implications. AJR Am J Roentgenol 1995;164:421-8.
32. Russ PD, Pretorius DH, Manco-Johnson ML, Rumack CM. The fetal spine. Neuroradiology 1986;28:398-407.
33. Filly RA, Golbus MS. Ultrasonography of the normal and pathologic fetal skeleton. Radiol Clin North Am 1982;20:311-23.
34. McCollough CH, Primak AN, Braun N, Kofler J, Yu L, Christner J. Strategies for reducing radiation dose in CT. Radiol Clin North Am 2009;47:27-40.
35. Coleman BG, Langer JE, Horii SC. The diagnostic features of spina bifida: the role of ultrasound. Fetal Diagn Ther 2015;37:179-96.
36. Likert R. A technique for the measurement of attitudes. Arch Psychol 1932;22:55.
37. Griffiths PD, Bradburn M, Campbell MJ, Cooper CL, Graham R, Jarvis D, Kilby MD, Mason G, Mooney C, Robson SC, Wailoo A; MERIDIAN collaborative group. Use of MRI in the diagnosis of fetal brain abnormalities

in utero (MERIDIAN): a multicentre, prospective cohort study. Lancet 2017;389:538-46.
38. Sherrod BA, Ho WS, Hedlund A, Kennedy A, Ostrander B, Bollo RJ. A comparison of the accuracy of fetal MRI and prenatal ultrasonography at predicting lesion level and perinatal motor outcome in patients with myelomeningocele. Neurosurg Focus 2019;47:E4.
39. Di Mascio D, Greco F, Rizzo G, Khalil A, Buca D, Sorrentino F, Vasciaveo L, Greco P, Nappi L, D'Antonio F. Diagnostic accuracy of prenatal ultrasound in identifying the level of the lesion in fetuses with open spina bifida: A systematic review and meta-analysis. Acta Obstet Gynecol Scand 2021;100:210-9.
40. Griffiths PD, Widjaja E, Paley MN, Whitby EH. Imaging the fetal spine using in utero MR: diagnostic accuracy and impact on management. Pediatr Radiol 2006;36:927-33.
41. Eyüboğlu İ, Dinç G. Fetal US and MRI in detection of craniospinal anomalies with postnatal correlation: single-center experience Turk J Med Sci 2021;51:1211-9.
42. Fischer R, Glob. libr. women's med. Amniotic Fluid: Physiology and Assessment. 2008.
43. Yanagihara T, Hata T. Three-dimensional sonographic visualization of fetal skeleton in the second trimester of pregnancy. Gynecol Obstet Invest 2000;49:12-6.
44. Sonel B, Yalçin P, Oztürk EA, Bökesoy I. Butterfly vertebra: a case report. Clin Imaging 2001;25:206-8.
45. Hedequist D, Emans J. Congenital scoliosis: a review and update. J Pediatr Orthop 2007;27:106-16.
46. Tanaka T, Uhthoff HK. Coronal cleft of vertebrae, a variant of normal enchondral ossification. Acta Orthop Scand 1983;54:389-95.
47. Ulla M, Aiello H, Cobos MP, Orioli I, García-Mónaco R, Etchegaray A, Igarzábal ML, Otaño L. Prenatal diagnosis of skeletal dysplasias: contribution of three-dimensional computed tomography. Fetal Diagn Ther 2011;29:238-47.
48. Whyte MP, Greenberg CR, Salman NJ, Bober MB, McAlister WH, Wenkert D, et al. Enzyme-replacement therapy in life-threatening hypophosphatasia. N Engl J Med 2012;366:904-13.
49. Gonçalves LF, Lee W, Mody S, Shetty A, Sangi-Haghpeykar H, Romero R. Diagnostic accuracy of ultrasonography and magnetic resonance imaging for the detection of fetal anomalies: a blinded case-control study. Ultrasound Obstet Gynecol 2016;48:185-92.
50. Ng CS, Palmer CR. Analysis of diagnostic confidence and diagnostic accuracy: a unified framework. Br J Radiol 2007;80:152-60.

Cite this article as: Cai X, Chen X, Wei X, Liu W, Hou X, Gong T, Zhu J, Haacke EM, Wang G. Use of magnetic resonance imaging in the diagnosis of fetal vertebral abnormalities in utero: a single-center retrospective cohort study. Quant Imaging Med Surg 2022;12(6):3391-3405. doi: 10.21037/qims-21-1070

Supplementary

Table S1 A full summary of all fetal diagnoses, imaging findings on US and MRI and postnatal diagnosis

Case number	Age (years)	Gestational age (weeks + days)	US diagnosis before referral for MRI	MRI diagnosis	Outcomes /follow-up
1	24y	25w	the lumbosacral part slightly curved; hemivertebrae?	(-)	(-)
2	29y	26w	T1, T3 vertebra morphological irregularity	(-)	(-)
3	29y	21w	MRI examination recommended to exclude thoracic abnormalities	(-)	(-)
4	29y	24w	the thoracic vertebra small in size	(-)	(-)
5	30y	25w	MRI examination recommended to exclude middle and lower thoracic abnormalities	(-)	(-)
6	34y	25w+3d	T11, T12 and L1 vertebral bodies slightly smaller	(-)	(-)
7	39y	26w	MRI examination recommended to exclude thoracic abnormalities	(-)	(-)
8	26y	26w+1d	T1, T2 vertebrae arranged irregularly	(-)	(-)
9	34y	26w+3d	T2, T3 vertebrae slightly out of order	(-)	(-)
10	32y	27w	normal, MRI examination recommended	(-)	(-)
11	29y	29w	T2 slightly larger in size	(-)	(-)
12	26y	30w	normal, MRI examination recommended	(-)	(-)
13	27y	30w+5d	the upper thoracic vertebrae arranged irregularly	(-)	(-)
14	33y	36w	normal, MRI examination recommended	(-)	(-)
15	24y	38w	the thoracic block vertebrae	(-)	(-)
16	21y	38w+3d	the sacrococcygeal abnormalities	(-)	(-)
17	31y	28w+1d	the thoracic vertebrae arranged irregularly	(-)	(-)
18	35y	26w	T2, T3 vertebrae body small in size	(-)	(-)
19	32y	28w	T8, T10 irregularity in morphology	(-)	(-)
20	29y	22w+5d	normal, MRI examination recommended	(-)	(-)
21	28y	29w	T12 arranged irregularly	(-)	(-)
22	30y	24w+5d	T8, T9, T10, L3, L4, L5 displayed unsatisfactory	(-)	(-)
23	27y	35w	T8, T9 slightly smaller	(-)	(-)
24	30y	24w	echo of the L1/2 vertebral arch enhanced	(-)	(-)
25	29y	26w+6d	normal, MRI examination recommended	(-)	(-)
26	31y	29w+5d	L2, L3, L4 irregularity in morphology	(-)	(-)
27	27y	36w	normal, MRI examination recommended	(-)	(-)
28	31y	27w+5d	C7 transverse process too long	(-)	(-)
29	27y	31w	normal; MRI examination recommended	(-)	(-)
30	38y	35w	the sacrococcygeal abnormalities	(-)	(-)
31	26y	25w	T5, T8 vertebrae body small in size	(-)	(-)

Table S1 (*continued*)

https://dx.doi.org/10.21037/qims-21-1070

Table S1 (*continued*)

Case number	Age (years)	Gestational age (weeks + days)	US diagnosis before referral for MRI	MRI diagnosis	Outcomes /follow-up
32	34y	26w	parts of vertebrae arranged irregularly	(-)	(-)
33	31y	34w	T4 irregularity in morphology	(-)	(-)
34	32y	28w+2d	C7, T3, T4 coronal clefts vertebrae?	(-)	(-)
35	26y	24w	L5 coronal cleft vertebra	(-)	(-)
36	26y	24w	normal, MRI examination recommended	(-)	(-)
37	33y	29w+6d	L2 irregularity in morphology	(-)	(-)
38	32y	28w	T4, T5 arranged irregularly	(-)	(-)
39	28y	31w	T10 vertebrae body small in size	(-)	(-)
40	31y	30w	the sacrococcygeal vertebrae arranged irregularly	(-)	(-)
41	33y	27w+1d	the sacrococcygeal vertebrae arranged irregularly	(-)	(-)
42	25y	32w+2d	the lumbosacral vertebrae arranged irregularly	(-)	(-)
43	37y	34w+6d	the upper thoracic vertebrae irregularity in morphology	(-)	(-)
44	32y	27w	thoracic hemivertebra?	(-)	(-)
45	23y	34w	the sacrococcygeal vertebrae poorly showed	(-)	(-)
46	37y	25w	T11 hemivertebra?	T11 hemivertebra?	(-)
47	39y	27w	T12 butterfly vertebra	T12 hemivertebra?	T11 butterfly vertebra
48	22y	24w	T11 butterfly vertebra	T11 butterfly vertebra	T11 butterfly vertebra
49	26y	24w	T11 butterfly vertebra	T11 butterfly vertebra	T11 butterfly vertebra
50	30y	25w	L5 butterfly vertebra?	L5 butterfly vertebra	L5 butterfly vertebra
51	23y	27w	T10 hemivertebra	T10 hemivertebra	T10 butterfly vertebra
52	31y	27w	T8 butterfly vertebra	T8 butterfly vertebra	T8 butterfly vertebra
53	32y	23w	L4 butterfly vertebra	L4 butterfly vertebra	L4 butterfly vertebra
54	38y	29w	T5 hemivertebra	T5 hemivertebra	T5 butterfly vertebra
55	37y	25w+5d	T10 butterfly vertebra?	T10 butterfly vertebra	T10 butterfly vertebra
56	25y	31w	T11 hemivertebra	T11 hemivertebra	T11 butterfly vertebra
57	34y	29w+4d	C5/6, C6/7 intervertebral space narrowing	T4 butterfly vertebra	T4 butterfly vertebra
58	22y	35w+2d	sacrococcygeal vertebra arranged irregularly	T3 butterfly vertebra	T3 butterfly vertebra
59	37y	26w	T10 butterfly vertebra	T10 butterfly vertebra	T10 butterfly vertebra
60	25y	28w	T11 hemivertebra?	T11 butterfly vertebra	T11 butterfly vertebra
61	34y	33w	T10 butterfly vertebra?	T10 butterfly vertebra	T10 butterfly vertebra
62	33y	26w	T9 butterfly vertebra	T9 butterfly vertebra	T9 butterfly vertebra
63	33y	24w	L3 butterfly vertebra?	L3 butterfly vertebra	L3 butterfly vertebra
64	33y	36w+3d	T11 butterfly vertebra	T11 butterfly vertebra	T11 butterfly vertebra

Table S1 (*continued*)

https://dx.doi.org/10.21037/qims-21-1070

Table S1 (*continued*)

Case number	Age (years)	Gestational age (weeks + days)	US diagnosis before referral for MRI	MRI diagnosis	Outcomes /follow-up
65	29y	27w	T8 hemivertebra	T8 butterfly vertebra	T8 butterfly vertebra
66	23y	32w	T1 irregularity in morphology	T1 hemivertebra	T1 hemivertebra; T3 butterfly vertebra
67	31y	27w	T3, T5, T7, T10 arranged irregularly	T7 butterfly vertebra; T10 hemivertebra	T2, T3, T5, T6, T7, T10 butterfly vertebra
68	34y	25w	L4 butterfly vertebra?	L4 coronal vertebral cleft	disappear
69	30y	29w+4d	L3, L5 coronal vertebral clefts	L3, L5 coronal vertebral clefts	disappear, L2 level fatty filum terminale
70	30y	30w	L2, L3 coronal vertebral clefts	L2, L3 coronal vertebral clefts	disappear; T9-13 vertebral level syringomyelia
71	32y	33w	L2-L5 coronal vertebral clefts	L2-L5 coronal vertebral clefts	disappear
72	32y	25w+6d	L2 butterfly vertebra?	L2 coronal vertebral cleft	disappear
73	22y	26w	L3 butterfly vertebra?	L3 coronal vertebral cleft	disappear
74	32y	34w	L3 coronal vertebral cleft	L3 coronal vertebral cleft	disappear
75	34y	29w	T3-T6, L1-L3 irregularity in morphology	T4-6, L1-3 coronal vertebral clefts	disappear
76	35y	28w+4d	T12-L4 irregularity in morphology	T12-L1, L3-L5 coronal vertebral clefts	disappear
77	26y	28w	L2, L4 arranged irregularly	L2, L4, L5 coronal vertebral clefts	disappear
78	32y	28w	T4, T8, L1 coronal vertebral clefts	T4, T8, L1 coronal vertebral clefts	disappear
79	31y	27w+4d	L3 coronal vertebral cleft	L3 coronal vertebral cleft	disappear
80	30y	30w+2d	normal, MRI examination recommended	L3 coronal vertebral cleft	disappear
81	26y	28w	T10 irregularity in morphology	T10 coronal vertebral cleft	disappear
82	29y	26w	T1-T5, L2-L4 irregularity in morphology	L2 coronal vertebral cleft	disappear
83	29y	34w	T8 coronal vertebral cleft	T8 coronal vertebral cleft	disappear
84	24y	29w	T5-T7, L1-L5 irregularity in morphology	L2, L4 coronal vertebral clefts	disappear
85	37y	30w	L2-L5 irregularity in morphology	L2-5 coronal vertebral clefts	disappear
86	36y	26w	L3 irregularity in morphology	L3 coronal vertebral cleft	disappear
87	22y	27w+ 2d	L1 butterfly vertebra	L1, L3-5 coronal vertebral clefts	disappear
88	30y	34w	T8 vertebra small in size	T8 coronal vertebral cleft	disappear
89	29y	25w	T7, L2, L4 ossification center abnormal	L2, L3, L5 coronal vertebral cleft	disappear

Table S1 (*continued*)

https://dx.doi.org/10.21037/qims-21-1070

Table S1 (*continued*)

Case number	Age (years)	Gestational age (weeks + days)	US diagnosis before referral for MRI	MRI diagnosis	Outcomes /follow-up
90	28y	25w+3d	lumbar hemivertebra	L3/4 intervertebral space narrowing	L3-4 block vertebra
91	44y	24w	L4 irregularity in morphology	L4 hemivertebra with fusing to one side of L3	L4 hemivertebra with fusing to one side of L3
92	34y	27w	T12 irregularity in morphology	T10 hemivertebra with fusing to one side of T9	T10 hemivertebra with fusing to one side of T9
93	30y	24w	L2 hemivertebra?	L2 hemivertebra with fusing to one side of L3	L2 hemivertebra with fusing to one side of L3
94	26y	24w	L3 vertebra small in size	L2 hemivertebra with fusing to one side of L3	L2 hemivertebra with fusing to one side of L3
95	27y	26w	cervical vertebra hemivertebra	cervical hemivertebra	cervical hemivertebra
96	34y	39w	caudal vertebra irregularity in morphology	L2 hemivertebra	L2 hemivertebra
97	27y	31w+1d	thoracic block vertebra	T7 hemivertebra	T7 hemivertebra
98	32y	28w	scoliosis	T11 hemivertebra	T10 hemivertebra
99	29y	30w+3d	S1 hemivertebra?	S1 hemivertebra	S1 hemivertebra, imperforate anus
100	29y	27w	L1 hemivertebra	L1 hemivertebra	L1 hemivertebra
101	31y	33w	sacrococcygeal vertebra not seen	L5 hemivertebra	L5 hemivertebra
102	35y	34w	T12 hemivertebra	T12 hemivertebra	T12 hemivertebra
103	30y	26w	L2 hemivertebra	L2 hemivertebra	L2 hemivertebra
104	31y	27w	L3 hemivertebra	L3 hemivertebra	L3 hemivertebra
105	26y	26w	L4 hemivertebra	L4 hemivertebra	L4 hemivertebra
106	20y	27w	vertebra irregularity in morphology	T11, L5 hemivertebra	T11, L5 hemivertebra
107	31y	26w	L2 hemivertebra	T7, L2 hemivertebra	T7, L2 hemivertebra
108	29y	21w+6d	thoracic hemivertebra	multiple hemivertebra in thoracolumbar vertebra	T3, T5, T7, T11 hemivertebrae; T8 hemivertebra with fusing to one side of T9; L2, L3 large in size
109	29y	34w	T5 hemivertebra	T5 butterfly vertebra T9 hemivertebra	T5 butterfly vertebra T9 hemivertebrae
110	36y	24w	T4, T9 hemivertebra T8 butterfly vertebra L1-2 block vertebrae	T9 butterfly vertebra; T4 hemivertebra; L1-2 block vertebrae	T8, T9 butterfly vertebrae T4 hemivertebra L2-3 block vertebrae
111	28y	28w+5d	T12-L1 block vertebrae T9 butterfly vertebra	T12-L1 block vertebrae T9 butterfly vertebra	L1-L2 block vertebrae; T10 butterfly vertebra; imperforate anus

Table S1 (*continued*)

https://dx.doi.org/10.21037/qims-21-1070

Table S1 (*continued*)

Case number	Age (years)	Gestational age (weeks + days)	US diagnosis before referral for MRI	MRI diagnosis	Outcomes /follow-up
112	31y	24w	spina bifida with meningocele; multiple vertebral deformities	spina bifida with meningocele; tethered cord; multiple hemivertebra, butterfly vertebra in thoracolumbar vertebra; multiple intercostal space narrowing on one side	bifida with meningocele; T4 butterfly vertebra; T5-6, T11-12 block vertebra; T7-9, L3-5 hemivertebra; T7-8 rib fused
113	29y	21w+6d	multiple vertebral deformities; hemivertebra?	T5, T11 hemivertebra T10 butterfly vertebra T8-9, L3-4 block vertebra	T3, T5, T7, T11 hemivertebrae; T10 butterfly vertebra; T8-9, L3-4 block vertebrae;
114	26y	29w	T6, T7 hemivertebrae?	T6, T7, T9 hemivertebrae and/or butterfly vertebra	T5, T7, T8 butterfly vertebrae; T6 hemivertebra
115	30y	24w	T11, T12 arranged irregularly	T11-12 block vertebra	T3 hemivertebra; T4, T8, T9 butterfly vertebrae; T11-12 block vertebra
116	26y	31w	cervical vertebral arranged irregularly	cervical vertebral body and appendix arranged irregularly	the congenital undescended scapula syndrome (sprengel deformity); cervical closed spina bifida
117	28y	23w+2d	multiple vertebral deformities with scoliosis	T6, T9 butterfly vertebra; T8 hemivertebra	T6, T9 butterfly vertebra; T8 hemivertebra
118	28y	25w	multiple vertebral deformities with scoliosis in upper thoracic	C6, T1 hemivertebra	C6, T1 hemivertebra; T2 butterfly vertebra
119	29y	22w	multiple vertebral deformities with scoliosis	multiple vertebral deformities	C6, C7, T3, T4 hemivertebra T1-2 block vertebra; T5 butterfly vertebra
120	23y	29w	vertebrae arranged irregularly in lower cervical and upper thoracic	T6-8 block vertebrae and/or hemivertebrae	T3 butterfly vertebra; T5-6, T11-12, L4-5 block vertebrae
121	27y	31w	the sacrococcygeal vertebrae poorly showed	anterior sacral meningocele (ASM); sacrococcygeal vertebra dysplasia;	anterior sacral meningocele (ASM): sacrococcygeal vertebra dysplasia; Caudal degeneration syndrome
122	32y	29w	low position of the conus medullaris	sacral vertebra dysplasia tethered cord meningocele	sacral agenesis tethered cord meningocele; Caudal degeneration syndrome
123	34y	25w+6d	the sacrococcygeal vertebra poorly showed; anus imperforate	sacral vertebra below S2 not visible	sacral agenesis: sacral vertebra below S2 not visible; anus imperforate; Caudal degeneration syndrome

Table S1 (*continued*)

https://dx.doi.org/10.21037/qims-21-1070

Table S1 (*continued*)

Case number	Age (years)	Gestational age (weeks + days)	US diagnosis before referral for MRI	MRI diagnosis	Outcomes /follow-up
124	31y	26w	the sacrococcygeal vertebrae showed poorly with thoracic hemivertebra	T9 hemivertebra sacral vertebrae below S1 not visible	T9 hemivertebra sacral vertebrae below S1 not visible; Caudal degeneration syndrome
125	26y	27w	the sacrococcygeal vertebra poorly showed	sacral vertebral below S1 not visible	sacral agenesis: sacral vertebrae below S1 not visible; Caudal degeneration syndrome
126	21y	30w	cervicothoracic vertebrae arranged irregularly	cervicothoracic vertebrae segmental spinal dysgenesis	cervicothoracic vertebrae segmental spinal dysgenesis
127	27y		scoliosis	scoliosis	scoliosis

US, ultrasound; MRI, magnetic resonance imaging.

https://dx.doi.org/10.21037/qims-21-1070